



Nitrogen speciation in various types of aerosols in spring over the northwestern Pacific Ocean

L. Luo¹, X. H. Yao², H. W. Gao², S. C. Hsu³, J. W. Li⁴, and S. J. Kao¹

¹State Key Laboratory of Marine Environmental Science, Xiamen University, Xiamen 361102, China

²Key laboratory of Marine Environmental Science and Ecology, Ministry of Education, Ocean University of China, Qingdao 266100, China

³Research Center for Environmental Changes, Academia Sinica, Taipei, Taiwan

⁴Key Laboratory of Regional Climate-Environment for Temperate East Asia, Institute of Atmospheric Physics, Chinese Academy of Sciences, Beijing 100029, China

Correspondence to: S. J. Kao (sjkao@xmu.edu.cn)

Received: 25 June 2015 – Published in Atmos. Chem. Phys. Discuss.: 18 September 2015

Revised: 4 December 2015 – Accepted: 13 December 2015 – Published: 18 January 2016

Abstract. The cumulative atmospheric nitrogen deposition has been found to profoundly impact the nutrient stoichiometry of the eastern China seas (ECSs: the Yellow Sea and East China Sea) and the northwestern Pacific Ocean (NWPO). In spite of the potential significance of dry deposition in those regions, shipboard observations of atmospheric aerosols remain insufficient, particularly regarding the compositions of water-soluble nitrogen species (nitrate, ammonium and water-soluble organic nitrogen – WSON). We conducted a cruise covering the ECSs and the NWPO during the spring of 2014 and observed three types of atmospheric aerosols. Aluminum content, air mass backward trajectories, weather conditions, and ion stoichiometry allowed us to discern dust aerosol patches and sea-fog-modified aerosols (widespread over the ECSs) from background aerosols (open ocean). Among the three types, sea-fog-modified aerosols contained the highest concentrations of nitrate ($536 \pm 300 \text{ nmol N m}^{-3}$), ammonium ($442 \pm 194 \text{ nmol N m}^{-3}$) and WSON ($147 \pm 171 \text{ nmol N m}^{-3}$); furthermore, ammonium and nitrate together occupied $\sim 65\%$ of the molar fraction of total ions. The dust aerosols also contained significant amounts of nitrate ($100 \pm 23 \text{ nmol N m}^{-3}$) and ammonium ($138 \pm 24 \text{ nmol N m}^{-3}$) which were obviously larger than those in the background aerosols (26 ± 32 for nitrate and $54 \pm 45 \text{ nmol N m}^{-3}$ for ammonium), yet this was not the case for WSON. It appeared that dust aerosols had less of a chance to come in contact with WSON during

their transport. In the open ocean, we found that sea salt (e.g., Na^+ , Cl^- , Mg^{2+}), as well as WSON, correlated positively with wind speed. Apparently, marine dissolved organic nitrogen (DON) was emitted from breaking waves. Regardless of the variable wind speeds from 0.8 to as high as 18 m s^{-1} , nitrate and ammonium, by contrast, remained in narrow ranges, implying that some supply and consumption processes of nitrate and ammonium were required to maintain such a quasi-static condition. Mean dry deposition of total dissolved nitrogen (TDN) for sea-fog-modified aerosols ($1090 \pm 671 \mu\text{mol N m}^{-2} \text{ d}^{-1}$) was 5 times higher than that for dust aerosols ($190 \pm 41.6 \mu\text{mol N m}^{-2} \text{ d}^{-1}$) and around 20 times higher than that for background aerosols ($56.8 \pm 59.1 \mu\text{mol N m}^{-2} \text{ d}^{-1}$). Apparently, spring sea fog on the ECSs played an important role in removing atmospheric reactive nitrogen from the Chinese mainland and depositing it into the ECSs, thus effectively preventing its seaward export to the NWPO.

1 Introduction

Anthropogenic reactive nitrogen (N_r) emissions have dramatically increased in the last few decades owing to rapidly growing populations and industry (Galloway et al., 2008). China is one of the largest producers and emitters of N_r in the world (N_r emission of 12.18 Tg yr^{-1} ; Reis et al., 2009). Inevitably, large amounts of N_r emanate into the adjacent

seas through various pathways. Through the atmosphere, annual nitrogen depositions into the eastern China seas (ECSs: the Yellow Sea and East China Sea) had been reported to be the same order of magnitude carried by the Yangtze River discharge (Nakamura et al., 2005; Zhang et al., 2007). Both observational data and global models revealed that both of the Chinese marginal seas and the northwestern Pacific Ocean (NWPO) are under the atmospheric influence of the Asian continent, which supplied significant amounts of anthropogenic N_r (Duce et al., 2008) and terrigenous materials (Jickells et al., 2005). The cumulative effect of atmospheric input in the past decades even altered the nutrient stoichiometry on a regional scale, including the Chinese marginal seas and the North Pacific Ocean (Kim et al., 2011; Kim et al., 2014).

To better constrain atmospheric deposition of N_r into the ocean over large spatial and temporal scales, modeling the transport and deposition of air pollutants is essential. Models of atmospheric nitrogen deposition include abundant parameters, such as local emission densities, particle size, deposition velocity, chemical processes and meteorological conditions (Liu et al., 2005; Guenther et al., 2006; Kanakidou et al., 2012). However, model accuracy strongly relies on the validation by observational data. Unfortunately, ship-board observations, particularly for an offshore gradient from marginal seas to the open sea, are still limited.

In the marginal seas of China, dust and fog storms are two common intermittent weather events during the transition period from a cold to a warm season (Sun et al., 2001; Zhang et al., 2009). Dust aerosols may serve as a carrier bringing significant amounts of terrigenous and anthropogenic fingerprints including trace elements (Duce et al., 1980) and N_r (Chen and Chen, 2008) from inland into the open sea via long-range transport. By contrast, sea fog is relatively stagnant and restricted on a spatial scale. Fog is the intermediate stage between precipitation and aerosol. Fog forms by the activation of particulates with subsequent growth and incorporation of other gases and particles (Cape et al., 2011). Fog droplets are smaller in size when compared to rain drops; however, concentrations of water-soluble species in fog water were not necessarily higher or lower than those of precipitation because of complicated chemical processes (Sasakawa and Uematsu, 2002; Watanabe et al., 2006; Jung et al., 2013). Inland fog chemistry has been well studied and its impacts on terrestrial ecosystems have been highlighted (Chang et al., 2002; Lange et al., 2003). Researchers have even designed experiments to investigate the differences in aerosol chemistry for pre- and post-fog formation periods to explore the inland fog impact on aerosol chemistry (Biswas et al., 2008; Safai et al., 2008). Fog, in fact, can be sampled only by specialized fog samplers; however, during aerosol sampling at sea there is no way to avoid fog once sea fog forms. Nevertheless, the effect of sea fog on aerosol chemistry has not yet been well studied, even less so in the coastal and marginal seas of China, where air pollution is serious. Therefore, com-

pared with inland fog and dust aerosols, we have less knowledge about sea fog chemistry and the aerosol chemistry under sea fog influence. This is the first investigation of N_r speciation and deposition of sea-fog-modified aerosols (aerosol collected under sea fog influence) on the marginal seas off a continent producing strong emissions.

Different types of aerosols may be composed of different amounts of nitrogen species based on their formation history (e.g., origin, flow path, reactions during transport). In this study, we sampled total suspended particulate (TSP) marine aerosols on a cruise crossing over the ECSs and NWPO during spring 2014. Water-soluble nitrogen species and ion characteristics among different aerosol types, including dust, background and sea-fog-modified aerosols, were investigated. These observational data promoted our understanding of the type-specific concentration and deposition of various nitrogen species and the role of sea fog on nitrogen scavenging. The data may aid in validating model outputs for the Asian region and potentially evaluate the framework of nitrogen and aerosol interactions in current models.

2 Materials and methods

2.1 Aerosol sample collection and chemical analyses

A total of 44 TSP samples were collected using a high-volume TSP aerosol sampler (TE-5170D; Tisch Environmental Inc.) during a research cruise on the R/V *Dongfanghong II* from 17 March to 22 April 2014. The cruise tracks (Fig. 1) covered the ECSs and the NWPO. The samples were taken at ~ 12 h intervals. To avoid self-contamination from the research vessel, we sampled only when the vessel was cruising; thus, the sampling interval was not exactly 12 h. Based on simultaneous 1 s particle number concentration measurements made using an optical particle sizer (TSI, USA), we found that ship plumes affected the TSP sampling occasionally during cruising (these data will be presented in a separate paper). We calculated the plume contribution to the measured volume particle concentration of PM_{10} during each TSP sampling (self-contamination) and the short-period contribution was less than 3%. Detailed sampling information including date, time period and locations for each sample are listed in Table S1 in the Supplement. Meteorological data (Fig. 2) including wind speed and direction, relative humidity (RH) and temperature were recorded onboard.

The cruise encountered sea fog in the first few days (orange shading in Fig. 2 for 17–19 March) and five samples (nos. 1–5) were collected. Surprisingly, sea fog occurred again on 21–22 April, while approaching land (samples nos. 43 and 44). During the fog events, high RH and slow wind speed were recorded (see orange shading in Fig. 2). The strong temperature gradient indicated that the sea fog formed owing to a cold air mass from land confronting warm

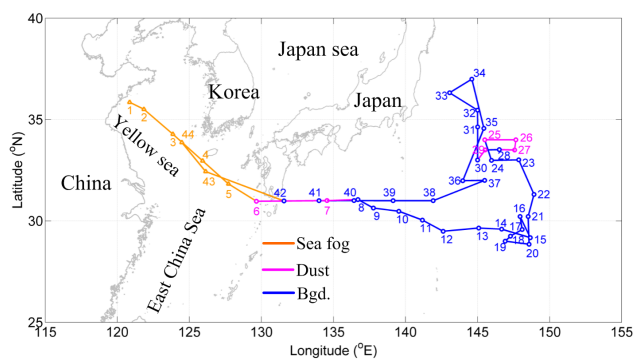


Figure 1. Map of the cruise track. Orange, pink and blue indicate sea fog, dust and background days during the cruise, respectively. Sample number and the collection range are shown.

air from the sea. Since these samples were collected on fog days (see orange tracks in Fig. 1) when we could collect aerosols, the sea-fog-modified aerosols as well as sea fog droplets. Since we could not separate them from each other through our method, we classified these samples as “sea-fog-modified aerosol”.

Whatman 41 cellulose filters (Whatman Limited, Maidstone, UK) were used for filtration. The analytical procedures were described by Hsu et al. (2010b, 2014). Briefly, one-eighth of the filter was extracted using 15 mL of Milli-Q water on a reciprocating shaker for 0.5 h and left to rest for an additional 0.5 h at room temperature. Then, the extract was filtered through a polycarbonate membrane filter (0.4 μm pore size and 47 mm in diameter from Nuclepore). The filter was leached three times with Milli-Q water, and then 5 mL of Milli-Q water was used to rinse the filter. The 45 mL extract solution was mixed with the 5 mL from rinsing, poured into a 50 mL clean plastic centrifuge tube and used for the determination of the ion species and water-soluble aluminum (Al).

The water-soluble and total concentrations of Al in the TSPs were analyzed using inductively coupled plasma mass spectrometers (ICP-MS). For total Al, briefly, one-eighth of the filter was digested with an acid mixture (4 mL HNO_3 + 2 mL HF) using an ultra-high-throughput microwave digestion system (MARSXpress, CEM Corporation, Matthews, NC, USA), and the efficiency of the digestion scheme was checked by subjecting a certain amount of a standard reference material (SRM1648, urban particulate matter, National Institute of Standards and Technology, USA) to the same treatment. The recoveries of Al in the SRM 1648 through digestion with the HNO_3 -HF mixture fell within $\pm 10\%$ ($n = 5$) of the certified values. Details regarding the ICP-MS analysis are described in Hsu et al. (2008).

The major ionic species (Na^+ , NH_4^+ , K^+ , Mg^{2+} , Ca^{2+} , Cl^- , NO_3^- , NO_2^- and SO_4^{2-}) in the extract were analyzed using an ion chromatograph (model ICS-1100 for anions

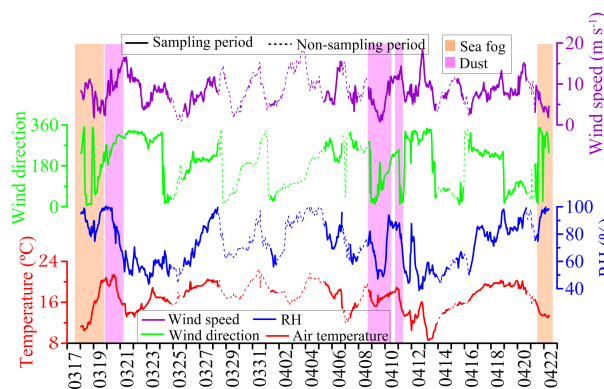


Figure 2. The meteorological parameters collected during the sampling period (solid line). Wind speed is in purple, wind direction in green, RH in blue and temperature in red. The orange shadings indicate the period of sea fog contact and pink indicate the dust period. Non-sampling period is shown with dashed curves.

and model ICS-900 for cations) equipped with a conductivity detector (ASRS-ULTRA) and suppressor (ASRS-300 for the ICS-1100 and CSRS-300 for the ICS-900). Separator columns (AS11-HC for anions and CS12A for cations) and guard columns (AG11-HC for anions and CG12A for cations) were used in the analyses. The precision for all ionic species was better than 5%. Details of the analytical processes can be found in Hsu et al. (2014). Only five samples contained NO_2^- (1.39 nmol m^{-3} for no. 2, 2.32 nmol m^{-3} for no. 4, 3.69 nmol m^{-3} for no. 5, 5.96 nmol m^{-3} for no. 43 and 3.76 nmol m^{-3} for no. 44), which accounted for $< 1\%$ of the total dissolved nitrogen (TDN).

The TDN was analyzed using the wet oxidation method to convert all nitrogen species into nitrate with recrystallized potassium persulfate, and then the concentration of nitrate was measured using chemiluminescence (Knapp et al., 2005). Monitoring with laboratory stock ($\text{NO}_3^- + \text{NH}_4^+ + \text{glycine} + \text{EDTA}$) showed that the recoveries of TDN by the persulfate oxidizing reagent (POR) digestion fell within 95–105% ($n = 6$) over the range of detection.

2.2 Data analysis

The amounts of non-sea-salt Ca^{2+} (nss- Ca^{2+}) and non-sea-salt SO_4^{2-} (nss- SO_4^{2-}) in the aerosol, as well as the Ca^{2+} and SO_4^{2-} fractions in excess over that expected from sea salt, were calculated using the unit of equivalent concentration (neq m^{-3}) in the following equations:

$$[\text{nss-Ca}^{2+}] = [\text{Ca}^{2+}] - [\text{ss-Ca}^{2+}],$$

$$\text{where } [\text{ss-Ca}^{2+}] = 0.044 \times [\text{Na}^+], \quad (1)$$

$$[\text{nss-SO}_4^{2-}] = [\text{SO}_4^{2-}] - [\text{ss-SO}_4^{2-}],$$

$$\text{where } [\text{ss-SO}_4^{2-}] = 0.121 \times [\text{Na}^+], \quad (2)$$

where the factors 0.044 and 0.121 are the typical calcium-to-sodium and sulfate-to-sodium equivalent molar ratios in seawater (Chester, 1990).

Relative acidity (RA) was calculated using all the observed ion species in their equivalent concentrations following Yao and Zhang (2012):

$$\text{RA} = ([\text{Na}^+] + [\text{Mg}^{2+}] + [\text{K}^+] + [\text{Ca}^{2+}] + [\text{NH}_4^+]) / ([\text{Cl}^-] + [\text{NO}_3^-] + [\text{SO}_4^{2-}]), \quad (3)$$

where $[\text{Na}^+]$, $[\text{Mg}^{2+}]$, $[\text{K}^+]$, $[\text{Ca}^{2+}]$, $[\text{NH}_4^+]$, $[\text{Cl}^-]$, $[\text{NO}_3^-]$ and $[\text{SO}_4^{2-}]$ are the equivalent concentrations of those water-extracted ions. The relative acidity is based on the imbalance of cations and anions, which was caused by the non-detected ions such as H^+ , HCO_3^- and CO_3^{2-} (Kerminen et al., 2001). When the total ions were distributed over a wide range (by a factor of 20 in our case), the ratio of total anions to cations in neq m^{-3} is more effective in presenting the relative acidity than the absolute value of imbalance (total cations – total anions).

The concentration of water-soluble organic nitrogen (WSON) was calculated using the following equation:

$$[\text{WSON}] = [\text{TDN}] - [\text{NO}_3^-] - [\text{NH}_4^+] - [\text{NO}_2^-], \quad (4)$$

where $[\text{TDN}]$, $[\text{NO}_3^-]$, $[\text{NH}_4^+]$ and $[\text{NO}_2^-]$ are molar concentrations (nmol N m^{-3}) of those water-soluble nitrogen species in TSPs. The standard errors propagated through WSON calculation varied from sample to sample (17 to 1500 %). The average standard error was 116 % when all samples were considered, and when the extreme value was excluded, the average standard error was reduced to 81 %.

2.3 Flux calculation

The dry deposition flux (F) was calculated by multiplying the aerosol concentrations of water-soluble nitrogen speciation (C) by the dry deposition velocity (V):

$$F = C \times V, \quad (5)$$

where V is a primarily function of particle size and meteorological parameters, such as wind speed, RH and sea surface roughness (Duce et al., 1991). According to previous reports, dry deposition velocity varies by more than 3 orders of magnitude at a particle size ranging from 0.1 to 100 μm (Hoppel et al., 2002). In general, ammonium appears in sub-micron mode from 0.1 to 1 μm , with a small fraction residing in the coarser mode; however, nitrate is mainly distributed in a supermicron size ranging from 1 to 10 μm (Nakamura et al., 2005; Baker et al., 2010; Yao and Zhang, 2012; Hsu

et al., 2014). The non-single-mode size distribution appears in not just nitrogenous elements but also metals, including aluminum and iron (e.g., Baker et al., 2013). Thus, for any compound or elements, using a fixed deposition velocity to calculate dry deposition flux might cause under- or over-estimation, as discussed by Baker et al. (2013). Unfortunately, we collected TSPs with no information for size distributions. Meanwhile, the meteorological parameters were highly variable during sample collection. In our observation wind speed ranging from 0.8 to 18 m s^{-1} under a RH ranging from 40 to 100 % (Fig. 2). Thus, it is very difficult to provide variable dry deposition velocities under a wide range of environmental conditions (Hoppel et al., 2002; Baker et al., 2013); thus, assumptions were made based on existing knowledge. Based on the model and experimental results for aerosol deposition to the sea surface (Duce et al., 1991; Hoppel et al., 2002) and the size distribution of nitrate and ammonium in particles as reported above, deposition velocity of 2 cm s^{-1} was applied for nitrate and 0.1 cm s^{-1} for ammonium. Both deposition velocities were often used in calculating the specific nitrogen deposition fluxes, especially for the maritime aerosols, though uncertainties were involved (de Leeuw et al., 2003; Nakamura et al., 2005; Chen et al., 2010; Jung et al., 2013). As for WSON, the size distribution of WSON in previous studies showed that WSON appears in a wide size spectrum (Chen et al., 2010; Lesworth et al., 2010; Srinivas et al., 2011). In previous studies, different orders of magnitude of deposition velocity were employed for WSON deposition (1.2 cm s^{-1} by He et al., 2011; 0.1 cm s^{-1} for fine and 1.0 cm s^{-1} for coarse by Srinivas et al., 2011; 0.075 cm s^{-1} for fine and 1.25 cm s^{-1} for coarse by Violaki et al., 2010). Our TSP aerosols covered the entire size distribution; thus, 1.0 cm s^{-1} was applied for WSON deposition. Since 1.0 cm s^{-1} is near the upper boundary of velocities previously applied for WSON deposition, our calculation of WSON deposition may represent the upper boundary.

Note that a period of our aerosol sampling was influenced by sea fog, which we could not avoid as mentioned earlier in the Introduction. Apparently, the deposition velocity for sea-fog-modified aerosol differs from that of common aerosol, thus, the deposition velocity needs to be revised once we have sufficient knowledge about the influence of sea fog on aerosol deposition.

2.4 Air mass backward trajectory analysis

In order to investigate the likely origins of aerosols in the transporting air masses, 3 days with three heights of above-sea-level air mass backward trajectories were calculated using the National Oceanic and Atmospheric Administration (NOAA) Hybrid Single Particle Lagrangian Integrated Trajectory (HYSPLIT) model with a $1^\circ \times 1^\circ$ latitude–longitude grid and the final meteorological database. Details about the HYSPLIT model can be found at <https://ready.arl.noaa.gov/HYSPLIT.php>, as prepared by the NOAA Air Resources

Laboratory. The time period of 3 days was suggested to be sufficient for dust transport from dust source to the NWPO (Husar et al., 2001). The three heights (100, 500 and 1000 m) were selected because 1000 m can be taken as one of the typical atmospheric boundary layers (Hennemuth and Lammert, 2006).

3 Results and discussion

Using the Al content, air mass backward trajectories, weather conditions, and ion stoichiometry, we classified aerosols into three types and then discussed the speciation and concentrations of N_r for each aerosol type as well as the potential processes involved. We compared the chemical characteristics of dust aerosols collected in the ECSs with ours under sea fog influence. Global aerosol and precipitation WSON data were also compiled to reveal the significance of WSON. Finally, we estimated the deposition of individual nitrogen species for the three types of aerosol and highlighted the importance of atmospheric nitrogen deposition in different regions.

3.1 Aerosol type classification

Total Al content in aerosol samples is an often used index to identify dust events (Hsu et al., 2008). As shown in Fig. 3, the total Al concentrations in aerosols ranged from 52 to 6293 ng m^{-3} during our entire cruise. For the first three samples (from nos. 1 to 3 collected in the Yellow Sea), total Al increased from 1353 to 6293 ng m^{-3} , and then rapidly decreased (nos. 4 and 5 in the East China Sea) as the cruise moved eastward to the NWPO (orange shading in Fig. 3). When the cruise returned to the ECSs, the total Al concentrations in the aerosols (nos. 43 and 44) increased once again. Apparently, an abundance of dust is frequently present in the low atmosphere over the Chinese marginal seas in spring. The air mass backward trajectories by HYSPLIT (Fig. 4a) revealed that the air masses for these fog samples mainly hovered over the ECSs at an altitude of $< 500 \text{ m}$ and the air masses for nos. 1–5 originated from the east coast of China. The air masses for the samples of nos. 43–44 were from southern South Korea. The water-soluble Al followed the same pattern as total Al (Fig. 3), but the leachable concentrations were significantly higher when compared with dust aerosols reported for the same area. The relative acidity of aerosols showed that the values of sea-fog-modified aerosols were all below 0.9 (Fig. 3), indicating an enhanced acidification relative to those aerosols with sea fog influence. The low RA values explained the higher concentrations of water-soluble Al.

As for sample nos. 6, 7, 25–27 and 29 collected in the NWPO (see pink tracks in Fig. 1), the total Al concentrations ranged from 590 to 1480 ng m^{-3} with an average of $1025 \pm 316 \text{ ng m}^{-3}$ (pink shading in Fig. 3), which were significantly higher than the remaining sam-

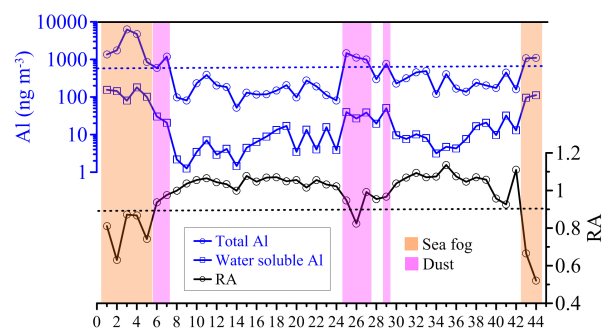


Figure 3. Total and water-soluble Al concentrations and relative acidity (RA) for TSP. The orange bars indicate the sea fog period, and the pink bars indicate the dust period. Sample identifications are shown on the x axis (see Table S1). The horizontal blue dashed line (590 ng m^{-3}) stands for the reference to define background aerosols, and black dashed line indicates the criterion of 0.9 for relative acidity.

ples ($212 \pm 120 \text{ ng m}^{-3}$) from the NWPO. Although most of the air mass backward trajectories of these samples collected in the NWPO originated from 25 to 40° N (and beyond) as well as high altitude (Fig. 4b), the lidar browse images from NASA (Fig. S1) clearly indicated that the air masses of these aerosol samples pass through dusty regions. The consistency between high total Al concentration and the occurrence of dust and polluted dust defined by the lidar browse images from the NASA allowed us to separate dust aerosols from background aerosols. In this paper, background aerosols stand for non-dusty and non-foggy aerosol in our classification. Thus, the background aerosol is more like a baseline aerosol collected within this study region during the investigating period; thus, the “background” may vary over space and time and it does not necessarily have to be pristine. Below we can also see a discernable ion stoichiometry among the three types.

3.2 Ion stoichiometry in three types of aerosol

Excluding sea-fog-modified aerosols, all the ratios of total anions and total cations followed close to a 1 : 1 linear relationship (Fig. 5a). Such a well-defined positive relationship indicated the charge balance and further emphasized the validity of our measurements. The sea-fog-modified aerosols in the ECSs contained higher contents of anions than cations, which was consistent with previous observations for fog water (Chang et al., 2002; Lange et al., 2003; Yue et al., 2014). The non-measured H^+ ion should be the dominant cation for charge compensation, as indicated previously (Chang et al., 2002; Lange et al., 2003). The low RA values for sea-fog-modified aerosols also supported this notion (Fig. 3). Below we set out the characteristics of the three types of aerosol with ion stoichiometry.

Since the $\text{Cl}^- / \text{Na}^+$ ratios of all samples including sea-fog-modified aerosols (Fig. 5b) were near 1.17, this indi-

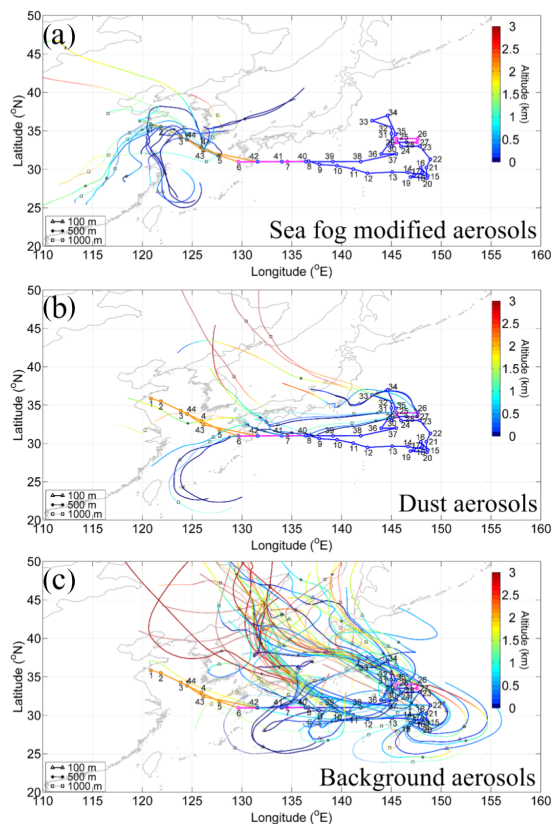


Figure 4. Map and cruise track superimposed on 3-day air mass backward trajectories corresponding to each sample. Altitudes of 100 m a.s.l. (triangles), 500 m a.s.l. (asterisks) and 1000 m a.s.l. (squares) are above sea level during the collection of (a) sea-fog-modified aerosols, (b) dust aerosols and (c) background aerosols. The color bar represents the altitude (in km).

cated that almost all the Na and Cl for our aerosols originated from sea salt. The relationship between Mg^{2+} vs. Na^+ (Fig. 5c) indicated that almost all Mg^{2+} also originated from sea salt sources ($\text{Mg}/\text{Na}_{\text{ss}} = 0.23$), except sea-fog-modified aerosols, which held a deviated correlation due to Mg enrichment ($y = 0.32x + 8.7$, $R^2 = 0.88$) because of terrestrial mineral sources of Mg. Such Mg enrichment was not observed in summer sea fog in the subarctic North Pacific Ocean (Jung et al., 2013).

As for Ca^{2+} (Fig. 5d), all types of aerosol were enriched in Ca^{2+} but at different levels, indicating various degrees of terrestrial mineral influence on the marine aerosols. For background aerosols, a strong correlation between Ca^{2+} and Na^+ ($y = 0.044x + 6.6$, $R^2 = 0.92$) was observed. The slope was identical to that of sea water ($\text{Ca}/\text{Na}_{\text{ss}} = 0.044$), suggesting that most Ca^{2+} and Na^+ in background aerosols were sourced from sea salt. An unusually high regression slope (20 times that of the sea salt) observed between Ca^{2+} and Na^+ in sea-fog-modified aerosols ($y = 0.90x - 1.8$, $R^2 = 0.71$) was attributable to the reaction between mineral CaCO_3 and H^+

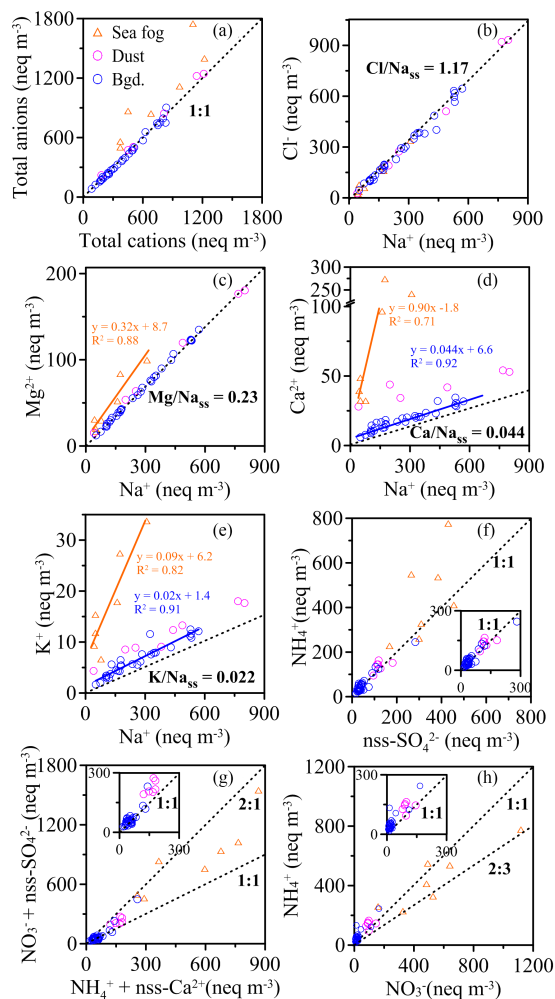


Figure 5. Scatter plots for equivalent concentrations of specific ions. (a) Total anions vs. total cations, (b) chloride vs. sodium, (c) magnesium vs. sodium, (d) calcium vs. sodium, (e) potassium vs. sodium, (f) ammonium vs. nss-sulfate, (g) $\sum(\text{nitrate} + \text{nss-sulfate})$ vs. $\sum(\text{nss-calcium} + \text{ammonium})$ and (h) nitrate vs. ammonium. Orange, pink and blue are for sea-fog-modified, dust and background aerosols, respectively.

in fog droplets during the formation of sea fog (Yue et al., 2012). The more excessive Ca^{2+} observed in dust aerosols implied that stronger heterogeneous reactions between the acid gas and dust minerals had occurred during long-range transport (Hsu et al., 2014). Similar to Ca^{2+} , patterns between K^+ and Na^+ can also be seen in Fig. 5e. However, besides the contribution from inland dust (Savoie and Prospero, 1980), excess K^+ may also originate from biomass burning in China (Hsu et al., 2009). Note that statistically significant intercepts could be seen in Ca^{2+} against Na_{ss} and K^+ against Na_{ss} scatter plots for background aerosols. Although small, such excesses in Ca^{2+} and K^+ relative to Na^+ in widespread background aerosols deserve further explanation.

As shown in Fig. 5f, a correlation was found between NH_4^+ and nss-SO_4^{2-} . Except for three sea fog samples, all ratios fell close to the 1 : 1 regression line, suggesting the dominance of $(\text{NH}_4)_2\text{SO}_4$ rather than NH_4HSO_4 . Complete neutralization of NH_4^+ by nss-SO_4^{2-} had likely occurred, and a similar phenomenon was found elsewhere (Zhang et al., 2013; Hsu et al., 2014).

The ratio of $[\text{NO}_3^- + \text{nss-SO}_4^{2-}]/[\text{NH}_4^+ + \text{nss-Ca}^{2+}]$ for background aerosols (Fig. 5g) closely followed unity, thus suggesting that $\text{NH}_4^+ + \text{nss-Ca}^{2+}$ was neutralized by the acidic ions NO_3^- and nss-SO_4^{2-} . However, for the dust and foggy aerosols, $[\text{NO}_3^- + \text{nss-SO}_4^{2-}]/[\text{NH}_4^+ + \text{nss-Ca}^{2+}]$ ratios located between 1 : 1 and 2 : 1 indicated that the excess anthropogenic acidic ions that originated from coal fossil fuel combustion and vehicle exhaust had been transported to the ECSs and NWPO by the Asian winter monsoon as previously indicated (Hsu et al., 2010a). On the other hand, Liu et al. (2013) suggested that NH_x emission in China is important and may play a major role in neutralizing the acidic ions. As shown in Fig. 5h, the scatter plot of NH_4^+ against NO_3^- , revealed that almost all dust and background aerosols sampled in the NWPO had $\text{NH}_4^+/\text{NO}_3^-$ ratios larger than 1, which is common in aerosol observation. However, significantly enriched NO_3^- in sea-fog-modified aerosols drew the ratio down to < 1 . Such high nitrate to ammonium ratios had been observed in a previous study of sea fog water collected from the South China Sea (Yue et al., 2012). In summary, the three types of aerosol had distinctive features in nitrogen speciation and ion stoichiometry including relative acidity (Fig. 6a), further supporting our aerosol type classification.

3.3 Nitrogen speciation and associated processes in different types of aerosol

3.3.1 Sea-fog-modified aerosols

Only a few studies concerning water-soluble nitrogen species in sea fog water have been published (Sasakawa and Uematsu, 2002; Yue et al., 2012; Jung et al., 2013). To the best of our knowledge, ours includes the first first-hand data from the Chinese marginal seas (the ECSs) in spring concerning water-soluble nitrogen species in aerosols collected under the influence of sea fog. As shown in Table 1 and Fig. 6a, in sea-fog-modified aerosols the concentrations of nitrate ranged from 160 to 1118 nmol N m^{-3} with a mean of $536 \pm 300 \text{ nmol N m}^{-3}$, and ammonium was slightly lower than nitrate, ranging from 228 to 777 nmol N m^{-3} with a mean of $442 \pm 194 \text{ nmol N m}^{-3}$. WSON in sea-fog-modified aerosols was the lowest nitrogen species ranging from 23 to 517 nmol N m^{-3} with a mean of $147 \pm 171 \text{ nmol N m}^{-3}$ (Table 1 and Fig. 6a). The sea-fog-modified aerosols contained 2–11 times higher concentration of nitrate, 2–6 times higher ammonium and 3–6 times higher WSON when compared with aerosols in the ECSs and other regions (Table 1). Such

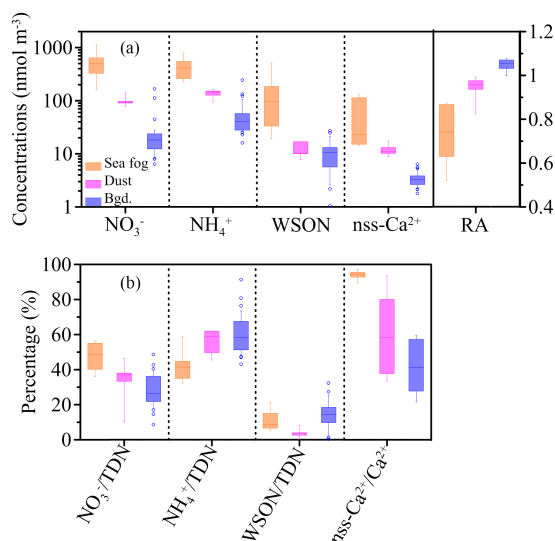


Figure 6. Box plots for (a) concentrations of NO_3^- , NH_4^+ , WSON and nss-Ca^{2+} , and RA, and (b) fractions of nitrogen species in total dissolved nitrogen and proportion of nss-Ca^{2+} in Ca^{2+} , in sea-fog-modified, dust and background aerosols. The large boxes represent the interquartile range from the 25th to 75th percentile. The line inside the box indicates the median value. The whiskers extend upward to the 90th and downward to the 10th percentile.

high concentrations of N_r not only highlighted the seriousness of the nitrogen air pollution in Chinese marginal seas but also underscored that water-soluble nitrogen species can be scavenged efficiently during sea fog formation.

Since no chemistry data of sea-fog-modified aerosols had been reported before, we can only compare with the dust aerosols from the same regions in spring. The concentrations of leachable ions, water-soluble Al, and total Al and RA for dust aerosols and sea-fog-modified aerosols sampled in the ECSs are listed in Table 2. The seven sea-fog-modified aerosols were distinctive in chemical characteristics. For all except NH_4^+ , NO_3^- and SO_4^{2-} , sea-fog-modified aerosols had lower or similar molar concentrations relative to dust aerosols. The anthropogenic species, particularly NO_3^- and NH_4^+ , were the most abundant ions in the sea-fog-modified aerosols. However, Na^+ and Cl^- were the highest among all the ions in dust aerosols from the island of Jeju and the East China Sea. Taking Jeju as an example, the concentration levels of Na^+ and Cl^- were similar to those of our sea-fog-modified aerosols, yet both NO_3^- and NH_4^+ in sea-fog-modified aerosols were > 6 times higher than those from the island of Jeju.

The pie charts for ion fractions of aerosols from the ECSs are shown in Fig. 7. Note that the fraction distribution of ions for the dust aerosols from a previous cruise in the ECSs ($n = 8$, Fig. 7b; Hsu et al., 2010b) resembled that collected from the island of Jeju ($n = 49$, Fig. 7c; Kang et al., 2009) despite the fact that their sampling was performed in different

Table 1. Nitrogen speciation in various aerosols reported from different regions.

Sample type	Date	Location		NO_3^- nmol m ⁻³	NH_4^+ nmol m ⁻³	WSON nmol m ⁻³	NO_3^- % ^a	NH_4^+ % ^a	WSON % ^a	Reference
TSP (sea fog)	Mar–Apr 2014	ECSs	Shelf	536 ± 300	442 ± 194	147 ± 171	48 ± 7	42 ± 9	10 ± 6	This study
TSP (dust)	Mar–Apr 2014	NWPO	Remote ocean	100 ± 23	138 ± 24	11.2 ± 4.0	41 ± 5	56 ± 7	5 ± 2	This study
TSP (bgd.)	Mar–Apr 2014	NWPO	Remote ocean	26 ± 32	54 ± 45	10.9 ± 6.8	27 ± 9	60 ± 11	14 ± 8	This study
TSP (dust)	Aug–Sep 2007, 2008	Barbados, Atlantic	Island	10 ± 4	11 ± 7	1.4 ± 1.3	45 ^c	49 ^c	6 ^c	Zamora et al. (2011)
TSP (dust)	May 2007–July 2009	Miami, FL, Atlantic	Coast city	28 ± 9	26 ± 10	3.0 ± 2.0	50 ^c	45 ^c	5 ^c	
PM _{>2} (dust)		Tropic Atlantic Ocean							14	Violaki et al. (2015)
TSP (dust)	Mar 2005–Apr 2007	Southwest ECS	Shelf	84 ± 98	177 ± 151	–	–	–	–	Hsu et al. (2010b)
TSP (dust)	Feb 1992–May 2004	Island of Jeju	Island	71 ± 44 ^c	72 ± 48 ^c	–	–	–	–	Kang et al. (2009)
TSP	Feb–Mar 2007	Northwest ECS	Shelf	68 ^c	193 ^c	–	–	–	–	Shi et al. (2010b)
TSP	Mar 2005–Apr 2007	Southwest ECS	Shelf	38 ± 45	89 ± 76	–	–	–	–	Hsu et al. (2010b)
TSP	Sep–Oct 2002	ECS	Shelf	34 ^c	136 ^c	54 ± 36	15 ^c	61 ^c	24	Nakamura et al. (2006)
TSP	Mar 2004	ECS	Shelf	39 ^c	91 ^c	16 ± 19	27 ^c	62 ^c	10	
TSP	Mar 2005, Apr 2006	Yellow Sea	Shelf	–	–	–	–	–	20	Shi et al. (2010a)
TSP	Apr 2010	Northwest ECS	Island	111 ^c	76 ^c	–	–	–	–	Zhu et al. (2013)
TSP	Mar 2011	Northwest ECS	Island	137 ^c	202 ^c	–	–	–	–	Zhu et al. (2013)
TSP	Spring 2003–2004	Northeast ECS	Island	85 ± 47 ^c	133 ± 78 ^c	–	–	–	–	Kundu et al. (2010)
TSP	Jul–Aug 2008	NWPO	Remote ocean	2.5	5.6	–	–	–	–	Jung et al. (2013)
TSP	Aug 2003–Sep 2005	Gulf of Aqaba	Coast	39 ± 19	25 ± 14	8 ± 5	53 ^c	34 ^c	11 ^c	Chen et al. (2007)
TSP	Nov–Dec 2000	Tasmania	Island	11 ± 7	2.6 ± 3.0	3.6 ± 5.7	63	15	21	Mace et al. (2003a)
TSP	Aug–Sep 2008	NWP	Remote ocean	1.8 ± 1.5	1.2 ± 1.1	1.1 ± 0.93	43 ^c	30 ^c	28 ^c	Miyazaki et al. (2011)
TSP	Apr 2007–Mar 2008	Marina, Singapore	Urban	50 ± 31 ^c	14 ± 8 ^c	56 ± 22 ^c	40 ± 15 ^c	11 ± 6 ^c	49 ± 17 ^c	He et al. (2011)
TSP	Jan–Dec 2006	Keelung, Taiwan	Coast city	–	–	76 ± 28	–	–	26 ^c	Chen et al. (2010)
TSP (sea spray)				6.7 ± 2.7	4.2 ± 1.7	0.5 ± 0.3	59 ^c	37 ^c	4 ^c	Zamora et al. (2011)
TSP (Bb) ^b				11 ± 11	18 ± 13	3.3 ± 2.0	34 ^c	56 ^c	10 ^c	
TSP (Bb) ^b				28 ± 16	48 ± 48	6.2 ± 6.4	34 ^c	58 ^c	8 ^c	Zamora et al. (2011)
TSP (pollution)				22 ± 11	23 ± 24	3.7 ± 2.8	45 ^c	48 ^c	8 ^c	
PM _{1,3–10}	2005, 2006	Crete, Greece	Island	26 ± 9	8.9 ± 4.0	5.5 ± 3.9	64	23	13	Violaki and Mihalopoulos (2010)
PM _{1,3}	2005, 2006	Crete, Greece		1.5 ± 1.3	70 ± 35	12 ± 14	2	85	13	
PM _{2,5}	Jan–Dec 2005	Indian Ocean	Remote ocean	0.3 ± 0.2	1.3 ± 1.0	0.8 ± 1.4	14	53	32	Violaki et al. (2015)
PM _{2,5–10}				0.2 ± 0.1	0.3 ± 0.1	0.2 ± 0.4	26	39	35	
PM _{2,5}	Jan 2007	Middle S. Atlantic	Remote ocean	–	–	1.3 ± 0.8	–	–	51	

^a Percentage in total dissolved nitrogen. ^b Bb indicates biomass burning. ^c Calculated value from the original data.

Table 2. Mean molar concentrations (nmol m^{-3}) of major ionic species together with Al (ng m^{-3}) in sea-fog-modified aerosols and dust aerosols in the ECS.

	Sea fog ^a mean \pm SD	Dust ^b mean \pm SD	Dust ^c mean \pm SD
Na^+	123.2 ± 97.5	294.8 ± 238.3	130.4 ± 85.2
NH_4^+	441.5 ± 193.9	177.6 ± 150.7	72.2 ± 47.7
Mg^{2+}	24.1 ± 16.5	41.2 ± 32.4	25.0 ± 12.9
K^+	17.5 ± 9.9	21.8 ± 19.1	17.9 ± 9.2
Ca^{2+}	54.7 ± 52.2	61.7 ± 39.5	76.9 ± 58.5
Cl^-	125.2 ± 111.3	280.9 ± 349.1	121.3 ± 101.6
NO_3^-	535.9 ± 299.7	83.6 ± 98.4	71.0 ± 43.5
SO_4^{2-}	172.5 ± 54.1	145.2 ± 103.2	104.0 ± 47.2
nss- SO_4^{2-}	165.1 ± 50.3	94.9 ± 89.0	96.1 ± 47.3
Total Al	2460 ± 2160	3470 ± 2730	4900 ± 6500
Water-soluble Al	124 ± 36	38 ± 45	nd
Al solubility	$5.0 \pm 1.7\%$	$1.1 \pm 1.6\%$	nd
Relative acidity	0.73 ± 0.13	1.07	1.06

^a This study; ^b Hsu et al. (2010b); ^c Derivation from Kang et al. (2009); nd: no data.

areas and at different times. Such consistency in the ion pie chart indicates the representativeness of these dust aerosols. However, the pie chart for sea-fog-modified aerosols revealed that NH_4^+ and NO_3^- occupied approximately 30 and 36 % of the total ionic concentration (Fig. 7a). Such an overwhelmingly high occupation of nitrogenous ions emphasizes the role of sea fog in modifying the chemistry of non-foggy dust aerosols.

In a previous study in the Po Valley, the average scavenging efficiencies for aerosol nitrate and ammonium were reported to be at similar levels (70 and 68 %; Gilardoni et al., 2014), while in our case the concentrations of nitrate in sea-fog-modified aerosols were higher than those of ammonium (Table 1 and Fig. 6a). Since the gas-phase HNO_3 is rapidly dissolved in liquid water particles during the early stages of fog formation (Fahey et al., 2005; Moore et al., 2004), it was reasonable to infer that the enriched nitrate in sea fog was attributed to gaseous HNO_3 owing to the gas–liquid equilibrium between NO_3^- and HNO_3 in fog droplets. Moreover, our sea-fog-modified aerosols were collected from the air masses moving around eastern China and the ECSs, where the NO_x emission is the highest in China (Gu et al., 2012). The lifetime of NO_x in the boundary layer is generally less than 2 days (Liang et al., 1998). Based on our air mass backward trajectories analysis, the travel time of air masses from inland China to the marginal seas is long enough for oxidation of NO_x into HNO_3 . Thus, nitrate enrichment in the sea-fog-modified aerosol was likely a synergistic consequence due to the sea fog formation and gas–liquid equilibrium of gaseous HNO_3 .

As for SO_4^{2-} , both the concentration and percentage occupation were comparable in sea-fog-modified aerosols and dust aerosols (Table 2 and Fig. 7). However, the concentrations of nss- SO_4^{2-} in sea-fog-modified aerosols were 60 %

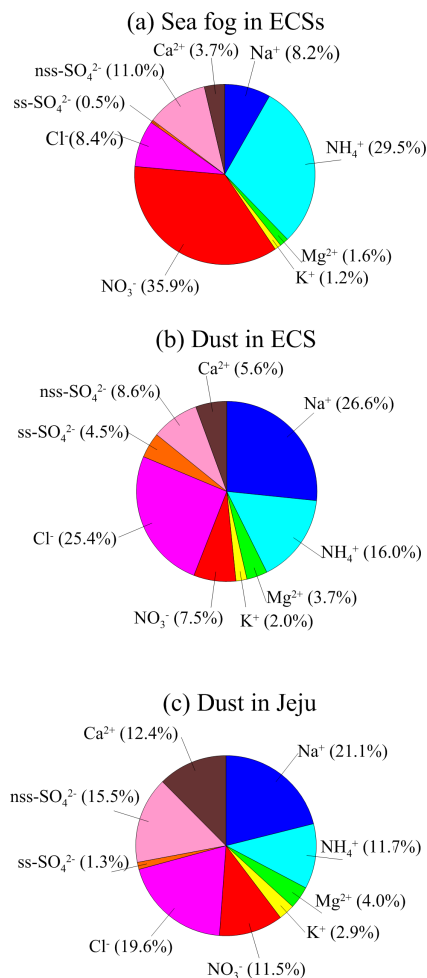


Figure 7. Pie charts of ion distribution for (a) sea-fog-modified aerosols (this study), (b) dust aerosols collected over the East China Sea ($n = 8$) (Hsu et al., 2010b), and (c) dust aerosols collected on the island of Jeju ($n = 49$) (Kang et al., 2009).

higher than those of dust aerosols (Table 2), suggesting the addition of anthropogenic SO_x emission during sea fog formation as indicated by Gilardoni et al. (2014). In the marginal seas adjacent to the anthropogenic emission source, acidified sea fog induced by additional sulfuric and nitric acid was common (Sasakawa and Uematsu, 2005; Yue et al., 2014).

In general, Al in marine aerosols originated from terrestrial minerals (Uematsu et al., 2010). The mean concentrations of total Al in our seven sea fog samples were the lowest among those in dust aerosols from the ECSs (Table 2). However, the concentrations as well as the fractions of water-soluble Al in sea-fog-modified aerosols were significantly higher than those of dust aerosols. Because of the high acidity (low RA values) for sea-fog-modified aerosols (Fig. 6a), we suspected that during the seasonal transition period the formation of sea fog at the land–ocean boundary may acidify

the aerosol to effectively promote the solubility of metals in aerosol minerals.

Finally, it has been shown that dissolved organic matter can be scavenged by fog, but its scavenging efficiency was lower than those of nitrate and ammonium due to hydrophobic organic species being more difficult to scavenge than hydrophilic ones (Maria and Russell, 2005; Gilardoni et al., 2014). In our case, although concentrations of WSON in sea-fog-modified aerosols ($147 \pm 171 \text{ nmol N m}^{-3}$) were significantly higher than those of background aerosols, the ratio of WSON to TDN in sea-fog-modified aerosols ($10 \pm 6\%$) was similar to those (ranging from 10 to 24%) of background aerosols sampled in the ECSs (Table 1). Such a high WSON concentration but low WSON % in TDN in sea-fog-modified aerosols may indicate the lower scavenging efficiency of WSON relative to other nitrogen species or that its source region is different or both.

Note that all these aerosols in our study were sampled by using TSP. Conventional knowledge indicates that aerosol may act as a precursor for fog formation, but this does not necessarily mean all the aerosols we sampled were directly associated with fog. Nevertheless, we observed distinctive chemistry for this type of aerosol either comparing with aerosols sampled during the same cruise or comparing with “non-foggy” aerosols collected in the ECSs in previous study. More studies are needed to explore the effect of sea fog formation on aerosol chemistry.

3.3.2 Dust aerosols

For dust aerosols collected in the NWPO, nitrate ranged from 79 to $145 \text{ nmol N m}^{-3}$ with an average of $100 \pm 23 \text{ nmol N m}^{-3}$, and ammonium ranged from 94 to $163 \text{ nmol N m}^{-3}$ with an average of $138 \pm 24 \text{ nmol N m}^{-3}$ (Table 1 and Fig. 6a). Relative to background aerosols, both nitrate and ammonium were significantly higher in dust aerosols revealing the anthropogenic nitrogen fingerprint carried by the Asian dust outflow along with westerlies (Chen and Chen, 2008). Interestingly, dust aerosols contained a low concentration of WSON ($11.2 \pm 4.0 \text{ nmol N m}^{-3}$) resembling that of background aerosols (Table 1 and Fig. 6a). Moreover, dust aerosols held the lowest WSON fraction in total dissolved nitrogen among the three types (Table 1 and Fig. 6b). Based on the good correlation between nss-Ca^{2+} and WSON, previous studies demonstrated that dust can carry anthropogenic “nitrogen” activity into remote oceans and simultaneously promote the ratio of WSON/TDN in aerosol (Mace et al., 2003b; Lesworth et al., 2010; Violaki et al., 2010). However, in our case there was no correlation between WSON and nss-Ca^{2+} (not shown), likely illustrating that these aerosols had less chance to come in contact with WSON along their pathway from a high altitude, or that WSON had been scavenged during transport. However, the latter was less likely.

3.3.3 Background aerosols

For the 31 background aerosol samples, the mean concentrations of NO_3^- and NH_4^+ were 26 ± 32 and $54 \pm 45 \text{ nmol N m}^{-3}$ (Table 1). Both were 10 times higher than those collected in the same region during summer ($2.5 \pm 1.0 \text{ nmol N m}^{-3}$ for nitrate and $5.9 \pm 2.9 \text{ nmol N m}^{-3}$ for ammonium; Jung et al., 2011). The 10 times higher N_T for springtime background aerosols indicated that the “spring background” was not pristine at all. Such distinctive seasonality was ascribed to the origins of air mass, since in summer the air masses in our study area were mainly from the open ocean, while in spring the air masses came from the north-east of China through the Japanese Sea and Japan (Fig. 4c), where they were strongly influenced by anthropogenic nitrogen emission (Kang et al., 2010). The concentration of WSON in background aerosols was $10.9 \pm 6.8 \text{ nmol N m}^{-3}$, which fell within the wide range reported previously (~ 1 to 76 nmol N m^{-3} ; Table 1). In the open ocean, the WSON in aerosols may come from natural and anthropogenic sources. For example, the highest percentage of WSON in TDN in the southern Atlantic (84%) was attributed to high biological productivity (Violaki et al., 2015). Unfortunately, no marine biological data (i.e., special amines or amino acids as summarized by Cape et al., 2011) existed in our case to directly support marine-sourced aerosol WSON.

Nevertheless, our sampling cruise experienced a wide range of wind speed with variable sea salt contents during the collection of background aerosols. The correlations between ion content and wind speed may reveal some useful information as indirect evidence. Higher sea salt, e.g., Na^+ , Cl^- , and Mg^{2+} , appeared with higher wind speed conditions (Fig. 8a–c). Positive correlations can be seen although r -square values were small, possibly due to time-integrated sampling (~ 12 h) and averaged wind speed over the sampling period. The positive correlation illustrated that the emission of sea salt aerosols was driven by wind intensity as indicated by Shi et al. (2012). Except for WSON (Fig. 8d), which was consistent with sea-salt-associated ions, no statistically significant relationships can be derived from scatter plots of nitrate and ammonium against wind speed (Fig. 8e and f). An analogous tendency between WSON and sea salt ions suggested that WSON might come from the surface ocean. Since the concentration of dissolved organic nitrogen (DON) in surface sea water was less variable, ranging from 4.5 to $5.0 \mu\text{M}$ in the Pacific Ocean (Knapp et al., 2011), DON can be taken as a relatively constant component in surface sea water similar to Na^+ , Cl^- and Mg^{2+} . Very likely, breaking waves and sea spray brought DON into the atmosphere under higher wind speed. In fact, using free amino acids and urea compositions in the maritime aerosol, Mace et al. (2003a) indicated that live species in the sea surface microlayer may serve as a source of atmospheric organic nitrogen.

Compared with DON in the surface ocean, it is not possible that nitrate and ammonium in the surface seawater are a

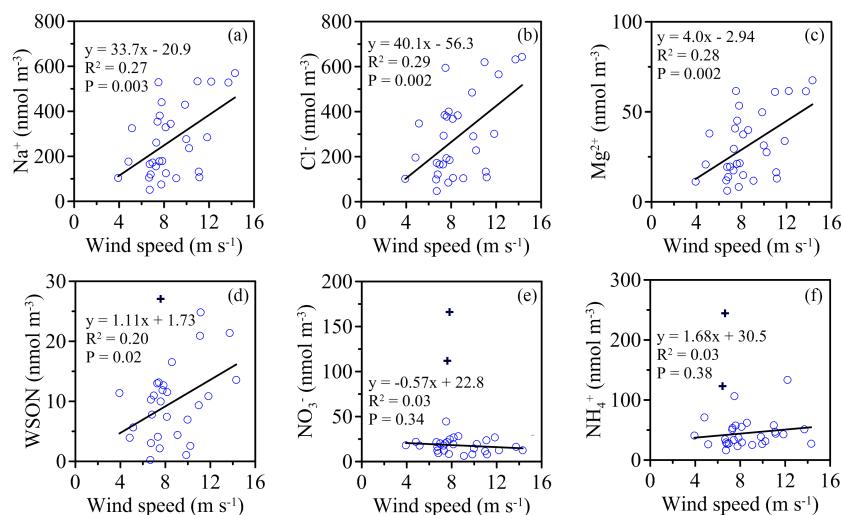


Figure 8. Scatter plots of concentrations of (a) Na⁺, (b) Cl⁻, (c) Mg²⁺, (d) WSON, (e) NO₃⁻, and (f) NH₄⁺ against corresponding wind speed for background aerosols. Wind speed was derived by averaging wind speed (5 min average) in corresponding sampling intervals. Crosses in (d), (e) and (f) were not considered during the linear regression.

source of atmospheric aerosol nitrate and ammonium since the concentrations of nitrate and ammonium are very low (a few tens to hundreds of nM) in the surface ocean. However, under a wide range of wind speed, we observed relatively narrow concentration ranges of aerosol ammonium and nitrate. This was strange, given that high wind speed implied vigorous exchange on the air–sea interface, during which both sea salt emission and scavenging were supposed to be high. Under efficient scavenging conditions, to maintain a relatively uniform aerosol nitrate or ammonium concentration (quasi-static), some supply processes are needed for compensation. Since the surface ocean is not a possible source for both aerosol ammonium and nitrate, we suggested alternative supplies which included deposition from the upper atmosphere and photochemical production/consumption.

Based on $\delta^{15}\text{N-NH}_4^+$ in aerosol (Jickells et al., 2003) and rainwater (Altieri et al., 2014) collected in the Atlantic, the ocean was suggested to be one of the ammonium sources for the atmosphere. Because of the low concentration of ammonium in the ocean surface, direct ammonium emission via sea spray was less likely. Based on our observation, we hypothesized that the emitted marine WSON in the atmosphere may serve as a precursor for ammonium and/or nitrate via the photodegradation and photooxidation processes reported previously (Spokes and Liss, 1996; Vione et al., 2005; Xie et al., 2012). A recent study by Paulot et al. (2015) supported our hypothesis. By modeling global inventories of ammonia emissions, they found that the ammonia source from the ocean cannot neutralize the sulfate aerosol acidity; thus photolysis of marine DON at the ocean surface or in the atmosphere was suggested to be a source of atmospheric ammonia. More studies about the exchange processes among nitro-

gen species through the ocean–atmosphere boundary layer are needed.

3.4 WSON in aerosol and rainwater: a global comparison

Organic nitrogen, distributed in the gas, particulate and dissolved phases, is an important component in the atmospheric nitrogen cycle. In our case, mean fractions of WSON in aerosol TDN were 10 ± 6 , 5 ± 2 and 14 ± 8 % for modified sea fog, dust and background aerosols, respectively. All values fell within the wide range reported previously (also in Table 1). Here we synthesized a published data set about aerosol WSON from around the world for comparison (Fig. 9a). The synthesized data revealed that aerosol WSON concentrations varied over 3 orders of magnitude and the fraction of WSON in TDN ranged from 1 % to as high as 85 %. Additionally, the fraction of WSON was the less variable towards high WSON concentrations. The slope of the linear regression between WSON and TDN indicated that WSON accounted for 18 % of aerosol TDN. Although the positive correlation between WSON and TDN may imply WSON's anthropogenic origin (Jickells et al., 2013), the marine-sourced WSON cannot be ignored in the open ocean as discussed in Sect. 3.3.3.

In Fig. 9b, we made a comparison between the distribution of the WSON fraction in rainwater TDN and that in aerosol. The distribution pattern of WSON fractions in aerosols (Fig. 9b, grey bar) was relatively concentrated, revealing a tendency towards lower fractions. Its peak frequency appeared at the category of 10–20 % and at least 80 % of the observed WSON fractions fell within < 25 %. However, for WSON/TDN in rainwater (Fig. 9b, blue bar),

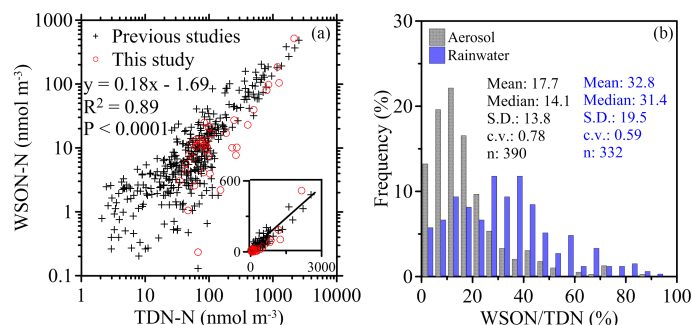


Figure 9. (a) Scatter plot of published aerosol WSON and TDN concentrations from around the world (red circles for this study, black crosses from Lesworth et al., 2010; Chen et al., 2007; Mace et al., 2003a; Miyazaki et al., 2011; Shi et al., 2010a; Srinivas et al., 2011; Zamora et al., 2011; and Violaki et al., 2015). (b) Frequency histograms for percentage WSON in aerosol TDN (grey bars, data from a) and in rainwater (blue bars, data from Cornell, 2011; Zhang et al., 2012; Altieri et al., 2012; Cui et al., 2014; Chen et al., 2015; and Yan and Kim, 2015).

the distribution pattern was relatively diffusive, shifting towards a higher percentage and peaking at around categories of 25–40% with a mean value of 33% ($n = 332$), which is slightly higher than that (24%, $n = 115$) obtained by Jickells et al. (2013). Although values of the coefficient of variation for both aerosol and rainwater were high, the results were still statistically meaningful. The mean WSON fraction for rainwater was around 2 times that for aerosol (18%), but the sampling bias inherent in such a comparison should be noted. In a previous study, Mace et al. (2003a) reported that the fractional contribution of dissolved free amino acids to organic nitrogen in rainwater was 4 times higher than that in aerosol. The higher fractional contribution of WSON to TDN for rainwater may imply that precipitation washed out hydrophilic organic matter or WSON from the atmosphere more effectively (Maria and Russell, 2005).

3.5 Dry deposition of TDN and the implications

As shown in Fig. 10, the atmospheric nitrogen dry deposition over the cruise revealed a large spatial variance under different weather conditions. In the ECSs, the mean DIN ($\text{NH}_4^+ + \text{NO}_3^-$) deposition on fog days was estimated to be $\sim 960 \mu\text{mol N m}^{-2} \text{d}^{-1}$ (926 ± 518 and $38 \pm 17 \mu\text{mol N m}^{-2} \text{d}^{-1}$ for nitrate and ammonium), which was around 6 times higher than the average values for ordinary aerosols derived from literature reports ($153 \mu\text{mol N m}^{-2} \text{d}^{-1}$ for aerosol nitrate and $12.3 \mu\text{mol N m}^{-2} \text{d}^{-1}$ for aerosol ammonium; see Table 3). The WSON deposition ranged from 20 to $446 \mu\text{mol N m}^{-2} \text{d}^{-1}$ with an average of $127 \pm 148 \mu\text{mol N m}^{-2} \text{d}^{-1}$. Since the bioavailability of aerosol WSON to phytoplankton was reported to be high (12–80%; Bronk et al., 2007; Wedyan et al., 2007), by taking WSON into consideration, the deposition of TDN will be $\sim 1100 \mu\text{mol N m}^{-2} \text{d}^{-1}$.

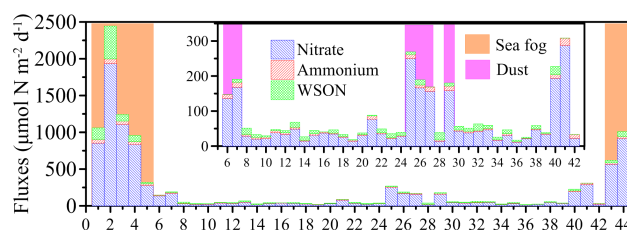


Figure 10. Dry deposition of aerosol nitrogen against sample identification. Nitrate is in blue, ammonium in red and WSON in green. Sample identifications, which match with Table S1, are shown on the x axis.

Taking $1150 \times 10^3 \text{ km}^2$ for the total area cover by the ECSs, we calculated the daily nitrogen supply from atmospheric deposition associated with sea fog to be $18 \pm 11 \text{ Gg TDN d}^{-1}$, which is around 6 times the nitrogen input from the Yangtze River in spring (total amount of $3.1 \text{ Gg DIN d}^{-1}$; Li et al., 2011) and 2 times the supply from the subsurface intrusion of the Kuroshio ($7.9 \text{ Gg NO}_3^- \text{ N d}^{-1}$; Chen, 1996). In the ECSs, the sea fog occurrence was around 3–5 days in March and 8–10 days in April (Zhang et al., 2009). Given such high TDN deposition per day, the contribution of foggy weather should really be taken into account in a monthly estimate even though the occurrence of sea fog is limited in time and space. Moreover, with a focus on the plume area, the atmospheric influence is more widespread than the river.

Assuming that nitrogen was the limiting nutrient and that all the total dissolved nitrogen deposited from atmosphere into the sea was bioavailable and would be utilized for carbon fixation, we obtained a C-fixation rate of $\sim 87 \text{ mg C m}^{-2} \text{d}^{-1}$ in spring for the ECSs based on the Redfield C/N ratio of 6.6. Since atmospheric nitrogen deposition is an external source, such a conversion represents new production. When compared with the primary productivity in the East China Sea ($292\text{--}549 \text{ mg C m}^{-2} \text{d}^{-1}$; Gong et al., 2000), the new

Table 3. The depositional fluxes reported or calculated for the Asian region and Pacific Ocean based on assumed deposition velocity.

Locations	Collection type	Date	NO ₃ ^{-a}	NH ₄ ⁺ ^a	WSON ^a	Total ^a	Reference
ECSs (sea fog)	Cruise	Mar–Apr 2014	926 ± 518	38 ± 17	127 ± 148	1090 ± 671	This study
NWPO (dust)	Cruise	Mar–Apr 2014	172 ± 40	11.9 ± 2.1	6.5 ± 5.7	190 ± 41.6	This study
NWPO (bgd.)	Cruise	Mar–Apr 2014	44.6 ± 55.3	4.66 ± 3.90	7.6 ± 6.5	56.8 ± 59.1	This study
Subarctic western North Pacific	Cruise	Jul–Aug 2008	3.3 ± 2.3	1.9 ± 0.63	–	5.3 ± 2.6	Jung et al. (2011)
Subtropical western North Pacific	Cruise	Aug–Sep 2008	3.0 ± 1.5	2.7 ± 2.1	–	5.7 ± 3.5	Jung et al. (2011)
Central North Pacific	Cruise	Jan 2009	1.6 ± 0.44	1.4 ± 0.96	–	3.1 ± 1.4	Jung et al. (2011)
Northwest ECS ^b	Cruise	Feb–Mar 2007	117	17	–	134	Shi et al. (2010b)
Southwest ECS ^b	Cruise	Spring 2005–2007	66	8	–	74	Hsu et al. (2010b)
Northwest ECS ^b	Coastal island	Apr 2010	192	6.6	–	198.6	Zhu et al. (2013)
Northwest ECS ^b	Coastal island	Mar 2011	237	17.5	–	254.5	Zhu et al. (2013)

^a In $\mu\text{mol N m}^{-2} \text{d}^{-1}$, ^b Recalculated fluxes based on assumed deposition velocity.

production associated with sea fog nitrogen deposition may account for 16–30 % of the primary production in the ECSs on foggy days in spring.

Similar to sea fog on the ECSs, sporadic dust events are frequently observed from March to May in the NWPO (Shao and Dong, 2006). In our spring case, the average deposition of dust aerosol nitrate and ammonium ($172 \pm 40 \mu\text{mol N m}^{-2} \text{d}^{-1}$ for nitrate and $11.9 \pm 2.1 \mu\text{mol N m}^{-2} \text{d}^{-1}$ for ammonium) were significantly higher than that of background aerosols ($44.6 \pm 55.3 \mu\text{mol N m}^{-2} \text{d}^{-1}$ for nitrate and $4.7 \pm 4.0 \mu\text{mol N m}^{-2} \text{d}^{-1}$ for ammonium; see Table 3). However, both dust and background aerosols depositions were significantly higher in spring when compared to summer dry deposition in the subtropical western North Pacific (3.0 ± 1.5 for nitrate and $2.7 \pm 2.1 \mu\text{mol N m}^{-2} \text{d}^{-1}$ for ammonium) and the subarctic western North Pacific (3.3 ± 2.3 for nitrate and $1.9 \pm 0.63 \mu\text{mol N m}^{-2} \text{d}^{-1}$ for ammonium) (Jung et al., 2011). Likewise, the C-fixation rate in the NWPO during spring was estimated to be $4.5\text{--}15 \text{ mg C m}^{-2} \text{d}^{-1}$ based on the above assumptions and observations. The minimal level of C fixation induced by dry deposition, in fact, equals to the maximum carbon uptake ($3.6 \text{ mg C m}^{-2} \text{d}^{-1}$; Jung et al., 2013) in summer by the total atmospheric DIN deposition (wet + dry + sea fog) in the western North Pacific Ocean. Thus, the contribution of atmospheric nitrogen deposition to primary production in the NWPO could be significantly different between seasons.

4 Conclusions

We presented the total dissolved nitrogen species including water-soluble organic nitrogen in TSP sampled over the ECSs and NWPO during spring and the samples of the ECSs were collected under sea fog influence. Three types of aerosol – the sea-fog-modified, dust and background aerosols – were classified. We found that sea fog formation significantly altered the aerosol chemistry, resulting in the highest concentrations of all nitrogen species among the three types of aerosol, accompanied by higher acidity and higher

cation deficiency. On a daily basis, the nitrogen supply from sea-fog-associated atmospheric deposition into the ECSs was around 6 times the nitrogen supply from the Yangtze River in spring (total amount of $3.1 \text{ Gg DIN d}^{-1}$) and 2 times the supply from the subsurface intrusion of Kuroshio ($7.9 \text{ Gg NO}_3^- \text{ N d}^{-1}$). Sea-fog-associated deposition and chemical processes require more attention and need to be considered in future aerosol monitoring and modeling works, especially in marginal seas during seasonal transition.

In the open sea, the spring background aerosol ammonium and nitrate were 10 times higher than previous report for summer, indicating an anthropogenic influence and the importance of the seasonality of the air mass source. The ammonium and nitrate varied in narrow ranges showing no correlation with wind speed, which may represent the degree of sea salt emission and scavenging. It is likely that nitrate and ammonium in the atmosphere above sea surface had reached a budget balance. Since the supply of nitrate and ammonium from surface ocean (bottom) is not possible, their sources might come from upper atmospheric boundary layer (top) or photochemical production of nitrogenous compounds. However, WSON revealed a similar pattern to the sea salt ions (Na^+ , Mg^{2+} and Cl^-), in which concentrations increased as the wind speed increased. Such a similarity indicated that at least a portion of the WSON should come from the surface ocean, where DON is emitted with sea salt. Future studies of nitrogen isotopic compositions of aerosol WSON and marine DON may shed light on the role of marine DON in nitrogen cycling of the air–sea interface.

The dust aerosols were significantly enriched in nitrate and ammonium, but not in WSON. Unless WSON-depletion processes had occurred, such a disproportionate enrichment suggests that dust aerosols from high latitude and altitude may have less chance to come in contact with WSON during long-range transport.

The WSON to TDN ratios of aerosols collected in the ECSs and NWPO fell within that of the global pattern of aerosols. Since nitrate and ammonium are mainly anthropogenic, the significantly positive correlation between WSON and TDN may imply WSON's anthropogenic origin.

When TDN concentrations were low ($< 100 \text{ nmol m}^{-3}$), the proportions of WSON in TDN were more diffusive, indicating that factors other than anthropogenic ones were involved. The mean ratio of WSON to TDN in aerosols was only 1/2 of that for precipitation over the world. Such a low proportion of WSON in aerosol TDN suggests that the aerosol was less capable of scavenging hydrophilic organic nitrogen when compared with precipitation. Nevertheless, WSON occupies a significant portion of the TDN for both aerosol and precipitation and thus cannot be overlooked in the atmospheric nitrogen cycle.

The Supplement related to this article is available online at doi:10.5194/acp-16-325-2016-supplement.

Acknowledgements. This research was funded by the Major State Basic Research Development Program of China (973 program) (nos. 2014CB953702 and 2015CB954003) and the National Natural Science Foundation of China (NSFC U1305233, 91328207 and 41121091). We also thank Peiran Yu and Tianfeng Guo (Ocean University of China) for helping us to collect samples during the cruise and Shuen-Hsin Lin (Academia Sinica in Taiwan) for help in chemical analyses. John Hodgkiss of the University of Hong Kong is thanked for his assistance with English.

Edited by: J. B. Burkholder

References

- Altieri, K. E., Hastings, M. G., Peters, A. J., Oleynik, S., and Sigman, D. M.: Isotopic evidence for a marine ammonium source in rainwater at Bermuda, *Global Biogeochem. Cy.*, 28, 1066–1080, 2014.
- Altieri, K. E., Hastings, M. G., Peters, A. J., and Sigman, D. M.: Molecular characterization of water soluble organic nitrogen in marine rainwater by ultra-high resolution electrospray ionization mass spectrometry, *Atmos. Chem. Phys.*, 12, 3557–3571, doi:10.5194/acp-12-3557-2012, 2012.
- Baker, A., Lesworth, T., Adams, C., Jickells, T., and Ganzeveld, L.: Estimation of atmospheric nutrient inputs to the Atlantic Ocean from 50° N to 50° S based on large-scale field sampling: Fixed nitrogen and dry deposition of phosphorus, *Global Biogeochem. Cy.*, 24, GB3006, doi:10.1029/2009GB003634, 2010.
- Baker, A., Adams, C., Bell, T., Jickells, T., and Ganzeveld, L.: Estimation of atmospheric nutrient inputs to the Atlantic Ocean from 50° N to 50° S based on large-scale field sampling: Iron and other dust-associated elements, *Global Biogeochem. Cy.*, 27, 755–767, 2013.
- Biswas, K., Ghauri, B., and Husain, L.: Gaseous and aerosol pollutants during fog and clear episodes in South Asian urban atmosphere, *Atmos. Environ.*, 42, 7775–7785, 2008.
- Bronk, D. A., See, J. H., Bradley, P., and Killberg, L.: DON as a source of bioavailable nitrogen for phytoplankton, *Biogeochemistry*, 4, 283–296, doi:10.5194/bg-4-283-2007, 2007.
- Cape, J. N., Cornell, S. E., Jickells, T. D., and Nemitz, E.: Organic nitrogen in the atmosphere—Where does it come from? A review of sources and methods, *Atmos. Res.*, 102, 30–48, 2011.
- Chang, S.-C., Lai, I.-L., and Wu, J.-T.: Estimation of fog deposition on epiphytic bryophytes in a subtropical montane forest ecosystem in northeastern Taiwan, *Atmos. Res.*, 64, 159–167, 2002.
- Chen, C.: The Kuroshio intermediate water is the major source of nutrients on the East China Sea continental shelf, *Oceanol. Acta*, 19, 523–527, 1996.
- Chen, H.-Y. and Chen, L.-D.: Importance of anthropogenic inputs and continental-derived dust for the distribution and flux of water-soluble nitrogen and phosphorus species in aerosol within the atmosphere over the East China Sea, *J. Geophys. Res.*, 113, D11303, doi:10.1029/2007jd009491, 2008.
- Chen, H. Y., Chen, L. D., Chiang, Z. Y., Hung, C. C., Lin, F. J., Chou, W. C., Gong, G. C., and Wen, L. S.: Size fractionation and molecular composition of water-soluble inorganic and organic nitrogen in aerosols of a coastal environment, *J. Geophys. Res.-Atmos.*, 115, D22307, doi:10.1029/2010JD014157, 2010.
- Chen, Y., Mills, S., Street, J., Golan, D., Post, A., Jacobson, M., and Paytan, A.: Estimates of atmospheric dry deposition and associated input of nutrients to Gulf of Aqaba seawater, *J. Geophys. Res.-Atmos.*, 112, D04309, doi:10.1029/2006JD007858, 2007.
- Chen, Y.-X., Chen, H.-Y., Wang, W., Yeh, J.-X., Chou, W.-C., Gong, G.-C., Tsai, F.-J., Huang, S.-J., and Lin, C.-T.: Dissolved organic nitrogen in wet deposition in a coastal city (Keelung) of the southern East China Sea: origin, molecular composition and flux, *Atmos. Environ.*, 112, 20–31, 2015.
- Chester, R.: *Marine Geochemistry*, Cambridge Univ. Press, London, 1990.
- Cornell, S. E.: Atmospheric nitrogen deposition: revisiting the question of the importance of the organic component, *Environ. Pollut.*, 159, 2214–2222, 2011.
- Cui, J., Zhou, J., Peng, Y., He, Y. Q., Yang, H., Xu, L. J., and Chan, A.: Long-term atmospheric wet deposition of dissolved organic nitrogen in a typical red-soil agro-ecosystem, Southeastern China, *Environ. Sci. Processes Impacts*, 16, 1050–1058, 2014.
- de Leeuw, G., Spokes, L., Jickells, T., Skjøth, C. A., Hertel, O., Vignati, E., Tamm, S., Schulz, M., Sørensen, L.-L., and Pedersen, B.: Atmospheric nitrogen inputs into the North Sea: effect on productivity, *Cont. Shelf Res.*, 23, 1743–1755, 2003.
- Duce, R., Unni, C., Ray, B., Prospero, J., and Merrill, J.: Long-range atmospheric transport of soil dust from Asia to the tropical North Pacific: temporal variability, *Science*, 209, 1522–1524, 1980.
- Duce, R., Liss, P., Merrill, J., Atlas, E., Buat-Menard, P., Hicks, B., Miller, J., Prospero, J., Arimoto, R., and Church, T.: The atmospheric input of trace species to the world ocean, *Global Biogeochem. Cy.*, 5, 193–259, 1991.
- Duce, R., LaRoche, J., Altieri, K., Arrigo, K., Baker, A., Capone, D., Cornell, S., Dentener, F., Galloway, J., and Ganeshram, R.: Impacts of atmospheric anthropogenic nitrogen on the open ocean, *Science*, 320, 893–897, 2008.
- Fahey, K., Pandis, S., Collett, J., and Herckes, P.: The influence of size-dependent droplet composition on pollutant processing by fogs, *Atmos. Environ.*, 39, 4561–4574, 2005.
- Galloway, J. N., Townsend, A. R., Erisman, J. W., Bekunda, M., Cai, Z., Freney, J. R., Martinelli, L. A., Seitzinger, S. P., and Sutton, M. A.: Transformation of the nitrogen cycle: recent trends, questions, and potential solutions, *Science*, 320, 889–892, 2008.

- Gilardoni, S., Massoli, P., Giulianelli, L., Rinaldi, M., Paglione, M., Pollini, F., Lanconelli, C., Poluzzi, V., Carbone, S., and Hillamo, R.: Fog scavenging of organic and inorganic aerosol in the Po Valley, *Atmos. Chem. Phys.*, 14, 6967–6981, doi:10.5194/acp-14-6967-2014, 2014.
- Gong, G.-C., Shiah, F.-K., Liu, K.-K., Wen, Y.-H., and Liang, M.-H.: Spatial and temporal variation of chlorophyll a, primary productivity and chemical hydrography in the southern East China Sea, *Cont. Shelf Res.*, 20, 411–436, 2000.
- Gu, B., Ge, Y., Ren, Y., Xu, B., Luo, W., Jiang, H., Gu, B., and Chang, J.: Atmospheric reactive nitrogen in China: sources, recent trends, and damage costs, *Environ. Sci. Technol.*, 46, 9420–9427, 2012.
- Guenther, A., Karl, T., Harley, P., Wiedinmyer, C., Palmer, P. I., and Geron, C.: Estimates of global terrestrial isoprene emissions using MEGAN (Model of Emissions of Gases and Aerosols from Nature), *Atmos. Chem. Phys.*, 6, 3181–3210, doi:10.5194/acp-6-3181-2006, 2006.
- He, J., Balasubramanian, R., Burger, D. F., Hicks, K., Kuylentstierna, J. C., and Palani, S.: Dry and wet atmospheric deposition of nitrogen and phosphorus in Singapore, *Atmos. Environ.*, 45, 2760–2768, 2011.
- Hennemuth, B. and Lammert, A.: Determination of the atmospheric boundary layer height from radiosonde and lidar backscatter, *Bound.-Lay. Meteorol.*, 120, 181–200, 2006.
- Hoppel, W., Frick, G., and Fitzgerald, J.: Surface source function for sea-salt aerosol and aerosol dry deposition to the ocean surface, *J. Geophys. Res.-Atmos.*, 107, AAC7.1–AAC7.17, doi:10.1029/2001JD002014, 2002.
- Hsu, S. C., Liu, S. C., Huang, Y. T., Lung, S. C. C., Tsai, F., Tu, J. Y., and Kao, S. J.: A criterion for identifying Asian dust events based on Al concentration data collected from northern Taiwan between 2002 and early 2007, *J. Geophys. Res.-Atmos.*, 113, D18306, doi:10.1029/2007JD009574, 2008.
- Hsu, S.-C., Liu, S. C., Huang, Y.-T., Chou, C. C. K., Lung, S. C. C., Liu, T.-H., Tu, J.-Y., and Tsai, F.: Long-range southeastward transport of Asian biomass pollution: signature detected by aerosol potassium in Northern Taiwan, *J. Geophys. Res.*, 114, D18306, doi:10.1029/2009jd011725, 2009.
- Hsu, S. C., Liu, S., Tsai, F., Engling, G., Lin, I., Chou, C., Kao, S., Lung, S., Chan, C., and Lin, S.: High wintertime particulate matter pollution over an off shore island (Kinmen) off southeastern China: an overview, *J. Geophys. Res.-Atmos.*, 115, D17309, doi:10.1029/2009JD013641, 2010a.
- Hsu, S.-C., Wong, G. T. F., Gong, G.-C., Shiah, F.-K., Huang, Y.-T., Kao, S.-J., Tsai, F., Candice Lung, S.-C., Lin, F.-J., Lin, I. I., Hung, C.-C., and Tseng, C.-M.: Sources, solubility, and dry deposition of aerosol trace elements over the East China Sea, *Mar. Chem.*, 120, 116–127, doi:10.1016/j.marchem.2008.10.003, 2010b.
- Hsu, S. C., Lee, C. S. L., Huh, C. A., Shaheen, R., Lin, F. J., Liu, S. C., Liang, M. C., and Tao, J.: Ammonium deficiency caused by heterogeneous reactions during a super Asian dust episode, *J. Geophys. Res.-Atmos.*, 119, 6803–6817, 2014.
- Husar, R. B., Tratt, D., Schichtel, B. A., Falke, S., Li, F., Jaffe, D., Gasso, S., Gill, T., Laulainen, N. S., and Lu, F.: Asian dust events of April 1998, *J. Geophys. Res.-Atmos.*, 106, 18317–18330, 2001.
- Jickells, T., Kelly, S., Baker, A., Biswas, K., Dennis, P., Spokes, L., Witt, M., and Yeatman, S.: Isotopic evidence for a marine ammonia source, *Geophys. Res. Lett.*, 30, 1374, doi:10.1029/2002GL016728, 2003.
- Jickells, T., An, Z., Andersen, K. K., Baker, A., Bergametti, G., Brooks, N., Cao, J., Boyd, P., Duce, R., and Hunter, K.: Global iron connections between desert dust, ocean biogeochemistry, and climate, *Science*, 308, 67–71, doi:10.1126/science.1105959, 2005.
- Jickells, T., Baker, A., Cape, J., Cornell, S., and Nemitz, E.: The cycling of organic nitrogen through the atmosphere, *Philos. T. R. Soc. B*, 368, 20130115, doi:10.1098/rstb.2013.0115, 2013.
- Jung, J., Furutani, H., and Uematsu, M.: Atmospheric inorganic nitrogen in marine aerosol and precipitation and its deposition to the North and South Pacific Oceans, *J. Atmos. Chem.*, 68, 157–181, doi:10.1007/s10874-012-9218-5, 2011.
- Jung, J., Furutani, H., Uematsu, M., Kim, S., and Yoon, S.: Atmospheric inorganic nitrogen input via dry, wet, and sea fog deposition to the subarctic western North Pacific Ocean, *Atmos. Chem. Phys.*, 13, 411–428, doi:10.5194/acp-13-411-2013, 2013.
- Kanakidou, M., Duce, R. A., Prospero, J. M., Baker, A. R., Benitez-Nelson, C., Dentener, F. J., Hunter, K. A., Liss, P. S., Mahowald, N., and Okin, G. S.: Atmospheric fluxes of organic N and P to the global ocean, *Global Biogeochem. Cy.*, 26, GB3026, doi:10.1029/2011GB004277, 2012.
- Kang, C.-H., Kim, W.-H., Ko, H.-J., and Hong, S.-B.: Asian dust effects on total suspended particulate (TSP) compositions at Gosan in Jeju Island, Korea, *Atmos. Res.*, 94, 345–355, 2009.
- Kang, J., Cho, B. C., and Lee, C.-B.: Atmospheric transport of water-soluble ions (NO_3^- , NH_4^+ and $\text{non-sulfate-SO}_4^{2-}$) to the southern East Sea (Sea of Japan), *Sci. Total Environ.*, 408, 2369–2377, 2010.
- Kerminen, V.-M., Hillamo, R., Teinilä, K., Pakkanen, T., Allegrini, I., and Sparapani, R.: Ion balances of size-resolved tropospheric aerosol samples: implications for the acidity and atmospheric processing of aerosols, *Atmos. Environ.*, 35, 5255–5265, 2001.
- Kim, I.-N., Lee, K., Gruber, N., Karl, D. M., Bullister, J. L., Yang, S., and Kim, T.-W.: Increasing anthropogenic nitrogen in the North Pacific Ocean, *Science*, 346, 1102–1106, 2014.
- Kim, T.-W., Lee, K., Najjar, R. G., Jeong, H.-D., and Jeong, H. J.: Increasing N abundance in the northwestern Pacific Ocean due to atmospheric nitrogen deposition, *Science*, 334, 505–509, 2011.
- Knapp, A. N., Sigman, D. M., and Lipschultz, F.: N isotopic composition of dissolved organic nitrogen and nitrate at the Bermuda Atlantic Time-series Study site, *Global Biogeochem. Cy.*, 19, GB1018, doi:10.1029/2004GB002320, 2005.
- Knapp, A. N., Sigman, D. M., Lipschultz, F., Kustka, A. B., and Capone, D. G.: Interbasin isotopic correspondence between upper-ocean bulk DON and subsurface nitrate and its implications for marine nitrogen cycling, *Global Biogeochem. Cy.*, 25, GB4004, doi:10.1029/2010GB003878, 2011.
- Kundu, S., Kawamura, K., and Lee, M.: Seasonal variation of the concentrations of nitrogenous species and their nitrogen isotopic ratios in aerosols at Gosan, Jeju Island: implications for atmospheric processing and source changes of aerosols, *J. Geophys. Res.-Atmos.*, 115, D20305, doi:10.1029/2009JD013323, 2010.
- Lange, C. A., Matschullat, J., Zimmermann, F., Sterzik, G., and Wienhaus, O.: Fog frequency and chemical composition of fog water—a relevant contribution to atmospheric deposition in the

- eastern Erzgebirge, Germany, *Atmos. Environ.*, **37**, 3731–3739, 2003.
- Lesworth, T., Baker, A. R., and Jickells, T.: Aerosol organic nitrogen over the remote Atlantic Ocean, *Atmos. Environ.*, **44**, 1887–1893, 2010.
- Li, X. A., Yu, Z., Song, X., Cao, X., and Yuan, Y.: Nitrogen and phosphorus budgets of the Changjiang River estuary, *Chin. J. Oceanol. Limn.*, **29**, 762–774, 2011.
- Liang, J. Y., Horowitz, L. W., Jacob, D. J., Wang, Y., Fiore, A. M., Logan, J. A., Gardner, G. M., and Munger, J. W.: Seasonal budgets of reactive nitrogen species and ozone over the United States, and export fluxes to the global atmosphere, *J. Geophys. Res.-Atmos.*, **103**, 13435–13450, 1998.
- Liu, X., Penner, J. E., and Herzog, M.: Global modeling of aerosol dynamics: model description, evaluation, and interactions between sulfate and nonsulfate aerosols, *J. Geophys. Res.-Atmos.*, **110**, D18206, doi:10.1029/2004JD005674, 2005.
- Liu, X., Zhang, Y., Han, W., Tang, A., Shen, J., Cui, Z., Vitousek, P., Erisman, J. W., Goulding, K., Christie, P., Fangmeier, A., and Zhang, F.: Enhanced nitrogen deposition over China, *Nature*, **494**, 459–462, doi:10.1038/nature11917, 2013.
- Mace, K. A., Duce, R. A., and Tindale, N. W.: Organic nitrogen in rain and aerosol at Cape Grim, Tasmania, Australia, *J. Geophys. Res.-Atmos.*, **108**, 4338, doi:10.1029/2002JD003051, 2003a.
- Mace, K. A., Kubilay, N., and Duce, R. A.: Organic nitrogen in rain and aerosol in the eastern Mediterranean atmosphere: an association with atmospheric dust, *J. Geophys. Res.-Atmos.*, **108**, 4320, doi:10.1029/2002JD002997, 2003b.
- Maria, S. F. and Russell, L. M.: Organic and inorganic aerosol below-cloud scavenging by suburban New Jersey precipitation, *Environ. Sci. Technol.*, **39**, 4793–4800, 2005.
- Miyazaki, Y., Kawamura, K., Jung, J., Furutani, H., and Uematsu, M.: Latitudinal distributions of organic nitrogen and organic carbon in marine aerosols over the western North Pacific, *Atmos. Chem. Phys.*, **11**, 3037–3049, doi:10.5194/acp-11-3037-2011, 2011.
- Moore, K. F., Sherman, D. E., Reilly, J. E., Hannigan, M. P., Lee, T., and Collett, J. L.: Drop size-dependent chemical composition of clouds and fogs. Part II: Relevance to interpreting the aerosol/trace gas/fog system, *Atmos. Environ.*, **38**, 1403–1415, 2004.
- Nakamura, T., Matsumoto, K., and Uematsu, M.: Chemical characteristics of aerosols transported from Asia to the East China Sea: an evaluation of anthropogenic combined nitrogen deposition in autumn, *Atmos. Environ.*, **39**, 1749–1758, 2005.
- Nakamura, T., Ogawa, H., Maripri, D. K., and Uematsu, M.: Contribution of water soluble organic nitrogen to total nitrogen in marine aerosols over the East China Sea and western North Pacific, *Atmos. Environ.*, **40**, 7259–7264, 2006.
- Paulot, F., Jacob, D. J., Johnson, M. T., Bell, T. G., Baker, A. R., Keene, W. C., Lima, I. D., Doney, S. C., and Stock, C. A.: Global oceanic emission of ammonia: Constraints from seawater and atmospheric observations, *Global Biogeochem. Cy.*, **29**, 1165–1178, doi:10.1002/2015GB005106, 2015.
- Reis, S., Pinder, R. W., Zhang, M., Lijie, G., and Sutton, M. A.: Reactive nitrogen in atmospheric emission inventories, *Atmos. Chem. Phys.*, **9**, 7657–7677, doi:10.5194/acp-9-7657-2009, 2009.
- Safai, P., Kewat, S., Pandithurai, G., Praveen, P., Ali, K., Tiwari, S., Rao, P., Budhawant, K., Saha, S., and Devara, P.: Aerosol characteristics during winter fog at Agra, North India, *J. Atmos. Chem.*, **61**, 101–118, 2008.
- Sasakawa, M. and Uematsu, M.: Chemical composition of aerosol, sea fog, and rainwater in the marine boundary layer of the northwestern North Pacific and its marginal seas, *J. Geophys. Res.-Atmos.*, **107**, ACH17.11–ACH17.19, 2002.
- Sasakawa, M. and Uematsu, M.: Relative contribution of chemical composition to acidification of sea fog (stratus) over the northern North Pacific and its marginal seas, *Atmos. Environ.*, **39**, 1357–1362, 2005.
- Savoie, D. and Prospero, J.: Water-soluble potassium, calcium, and magnesium in the aerosols over the tropical North Atlantic, *J. Geophys. Res.-Oceans*, **85**, 385–392, 1980.
- Shao, Y. and Dong, C.: A review on East Asian dust storm climate, modelling and monitoring, *Global Planet. Change*, **52**, 1–22, 2006.
- Shi, G., Li, Y., Jiang, S., An, C., Ma, H., Sun, B., and Wang, Y.: Large-scale spatial variability of major ions in the atmospheric wet deposition along the China Antarctica transect (31° N–69° S), *Tellus B*, **64**, 1–10, 2012.
- Shi, J., Gao, H., Qi, J., Zhang, J., and Yao, X.: Sources, compositions, and distributions of water-soluble organic nitrogen in aerosols over the China Sea, *J. Geophys. Res.-Atmos.*, **115**, D17303, doi:10.1029/2009JD013238, 2010a.
- Shi, J., Zhang, Y., Li, R., Gao, H., and Zhang, J.: Distributions of inorganic species in atmospheric over the East China Sea, *Environ. Sci.*, **31**, 2835–2843, 2010b (in Chinese).
- Spokes, L. J. and Liss, P. S.: Photochemically induced redox reactions in seawater, II. Nitrogen and iodine, *Mar. Chem.*, **54**, 1–10, 1996.
- Srinivas, B., Sarin, M., and Sarma, V.: Atmospheric dry deposition of inorganic and organic nitrogen to the Bay of Bengal: impact of continental outflow, *Mar. Chem.*, **127**, 170–179, 2011.
- Sun, J., Zhang, M., and Liu, T.: Spatial and temporal characteristics of dust storms in China and its surrounding regions, 1960–1999: Relations to source area and climate, *J. Geophys. Res.-Atmos.*, **106**, 10325–10333, 2001.
- Uematsu, M., Hattori, H., Nakamura, T., Narita, Y., Jung, J., Matsumoto, K., Nakaguchi, Y., and Kumar, M. D.: Atmospheric transport and deposition of anthropogenic substances from the Asia to the East China Sea, *Mar. Chem.*, **120**, 108–115, 2010.
- Violaki, K. and Mihalopoulos, N.: Water-soluble organic nitrogen (WSON) in size-segregated atmospheric particles over the Eastern Mediterranean, *Atmos. Environ.*, **44**, 4339–4345, doi:10.1016/j.atmosenv.2010.07.056, 2010.
- Violaki, K., Zarbas, P., and Mihalopoulos, N.: Long-term measurements of dissolved organic nitrogen (DON) in atmospheric deposition in the Eastern Mediterranean: fluxes, origin and biogeochemical implications, *Mar. Chem.*, **120**, 179–186, 2010.
- Violaki, K., Sciare, J., Williams, J., Baker, A. R., Martino, M., and Mihalopoulos, N.: Atmospheric water-soluble organic nitrogen (WSON) over marine environments: a global perspective, *Biogeosciences*, **12**, 3131–3140, doi:10.5194/bg-12-3131-2015, 2015.
- Vione, D., Maurino, V., Minero, C., and Pelizzetti, E.: Reactions induced in natural waters by irradiation of nitrate and nitrite ions,

- in: *Environmental Photochemistry Part II*, Springer, 221–253, 2005.
- Watanabe, K., Takebe, Y., Sode, N., Igarashi, Y., Takahashi, H., and Dokiya, Y.: Fog and rain water chemistry at Mt. Fuji: A case study during the September 2002 campaign, *Atmos. Res.*, 82, 652–662, doi:10.1016/j.atmosres.2006.02.021, 2006.
- Wedyan, M., Fandi, K., and Al-Rousan, S.: Bioavailability of atmospheric dissolved organic nitrogen in the marine aerosol over the Gulf of Aqaba, *Australian J. Basic Appl. Sci.*, 1, 208–212, 2007.
- Xie, H., Bélanger, S., Song, G., Benner, R., Taalba, A., Blais, M., Tremblay, J.-É., and Babin, M.: Photoproduction of ammonium in the southeastern Beaufort Sea and its biogeochemical implications, *Biogeosciences*, 9, 3047–3061, doi:10.5194/bg-9-3047-2012, 2012.
- Yan, G. and Kim, G.: Sources and fluxes of organic nitrogen in precipitation over the southern East Sea/Sea of Japan, *Atmos. Chem. Phys.*, 15, 2761–2774, doi:10.5194/acp-15-2761-2015, 2015.
- Yao, X. H. and Zhang, L.: Supermicron modes of ammonium ions related to fog in rural atmosphere, *Atmos. Chem. Phys.*, 12, 11165–11178, doi:10.5194/acp-12-11165-2012, 2012.
- Yue, Y., Niu, S., Zhao, L., Zhang, Y., and Xu, F.: Chemical Composition of Sea Fog Water Along the South China Sea, *Pure Appl. Geophys.*, 169, 2231–2249, doi:10.1007/s00024-012-0486-4, 2012.
- Yue, Y., Niu, S., Zhao, L., Zhang, Y., and Xu, F.: The influences of macro-and microphysical characteristics of sea-fog on fog-water chemical composition, *Adv. Atmos. Sci.*, 31, 624–636, 2014.
- Zamora, L., Prospero, J., and Hansell, D.: Organic nitrogen in aerosols and precipitation at Barbados and Miami: Implications regarding sources, transport and deposition to the western subtropical North Atlantic, *J. Geophys. Res.-Atmos.*, 116, D20309, doi:10.1029/2011JD015660, 2011.
- Zhang, G., Zhang, J., and Liu, S.: Characterization of nutrients in the atmospheric wet and dry deposition observed at the two monitoring sites over Yellow Sea and East China Sea, *J. Atmos. Chem.*, 57, 41–57, 2007.
- Zhang, R., Jing, J., Tao, J., Hsu, S.-C., Wang, G., Cao, J., Lee, C. S. L., Zhu, L., Chen, Z., Zhao, Y., and Shen, Z.: Chemical characterization and source apportionment of PM_{2.5} in Beijing: seasonal perspective, *Atmos. Chem. Phys.*, 13, 7053–7074, doi:10.5194/acp-13-7053-2013, 2013.
- Zhang, S.-P., Xie, S.-P., Liu, Q.-Y., Yang, Y.-Q., Wang, X.-G., and Ren, Z.-P.: Seasonal variations of Yellow Sea fog: observations and Mechanisms*, *J. Climate*, 22, 6758–6772, doi:10.1175/2009jcli2806.1, 2009.
- Zhang, Y., Song, L., Liu, X., Li, W., Lü, S., Zheng, L., Bai, Z., Cai, G., and Zhang, F.: Atmospheric organic nitrogen deposition in China, *Atmos. Environ.*, 46, 195–204, 2012.
- Zhu, L., Chen, Y., Guo, L., and Wang, F.: Estimate of dry deposition fluxes of nutrients over the East China Sea: the implication of aerosol ammonium to non-sea-salt sulfate ratio to nutrient deposition of coastal oceans, *Atmos. Environ.*, 69, 131–138, doi:10.1016/j.atmosenv.2012.12.028, 2013.